# Coupling of tandem Smad ubiquitination regulatory factor (Smurf) WW domains modulates target specificity

P. Andrew Chong[a], Hong Lin[a], Jeffrey L. Wrana[b,c], and Julie D. Forman-Kay[a,d,1]

[a]Program in Molecular Structure and Function, Hospital for Sick Children, 555 University Avenue, Toronto, ON, Canada M5G 1X8; [b]Department of Medical Genetics and Microbiology, University of Toronto, Toronto, ON, Canada M5S 1A8; [c]Samuel Lunenfeld Research Institute, Mt. Sinai Hospital, 600 University Avenue, Toronto, ON, Canada M5G 1X5; and [d]Department of Biochemistry, University of Toronto, Toronto, ON, Canada M5S 1A8

Edited by Aaron Ciechanover, Technion-Israel Institute of Technology, Bat Galim, Haifa, Israel, and approved August 25, 2010 (received for review March 9, 2010)

**Smad ubiquitination regulatory factor 2 (Smurf2) is an E3 ubiquitin ligase that participates in degradation of TGF-β receptors and other targets. Smurf2 WW domains recognize PPXY (PY) motifs on ubiquitin ligase target proteins or on adapters, such as Smad7, that bind to E3 target proteins. We previously demonstrated that the isolated WW3 domain of Smurf2, but not the WW2 domain, can directly bind to a Smad7 PY motif. We show here that the WW2 augments this interaction by binding to the WW3 and making auxiliary contacts with the PY motif and a novel E/D-S/T-P motif, which is N-terminal to all Smad PY motifs. The WW2 likely enhances the selectivity of Smurf2 for the Smad proteins. NMR titrations confirm that Smad1 and Smad2 are bound by Smurf2 with the same coupled WW domain arrangement used to bind Smad7. The analogous WW domains in the short isoform of Smurf1 recognize the Smad7 PY peptide using the same coupled mechanism. However, a longer Smurf1 isoform, which has an additional 26 residues in the inter-WW domain linker, is only partially able to use the coupled WW domain binding mechanism. The longer linker results in a decrease in affinity for the Smad7 peptide. Interdomain coupling of WW domains enhances selectivity and enables the tuning of interactions by isoform switching.**

Cellular signaling depends on interactions between modular binding domains and defined sequence motifs. For example, HECT-type E3 ubiquitin ligases utilize group I WW domains to recognize sequence motifs on many of their targets (1). WW domains, which are named for two highly conserved tryptophan residues, are composed of a single three stranded β-sheet. The first conserved tryptophan lies on one side of the sheet in the hydrophobic core and is required for domain stability (2), whereas the second tryptophan lies on the opposite side of the sheet in a target binding pocket. Group I WW domains, the most common type, generally recognize a PPXY sequence known as the PY motif. The binding pocket tryptophan participates in recognition of the prolines in the PY motif (3). Most HECT-type E3 ubiquitin ligases have multiple WW domains, suggesting that multiple WW domains are required to enhance target binding affinity through an "avidity" effect. In some cases, such as Rsp5p, Nedd4, and FBP11, more than one of the WW domains can bind to the same target (4–8), which is consistent with this hypothesis. The two consecutive WW domains of FBP11 are both able to individually bind to polyproline target motifs with modest affinity; however, in tandem they bind to a ligand containing two target motifs with much higher affinity. NMR data and molecular modeling suggest that the two FBP11 WW domains bind to the two target motifs in the ligand simultaneously (7). Although avidity or multiple target recognition sometimes explains the requirement for multiple WW domains, an alternate explanation is required for the Smad ubiquitination regulatory factor (Smurf) proteins.

Smurf1 and Smurf2 are HECT-type E3 ubiquitin ligases that are involved in down-regulation of the TGF-β signaling pathway (9, 10). Signals from TGF-β morphogens regulate key developmental processes through control of growth and differentiation of a variety of cell types. TGF-β signals are transmitted to the nucleus via the receptor regulated Smads (R-Smads) 1, 2, 3, 5, and 8 and the common Smad4 (11, 12) and inhibited by the inhibitory Smads (I-Smads) 6 and 7 (13). In addition to a C2 and a HECT domain, the Smurf proteins contain multiple WW domains, which are responsible for binding to PY motifs found in their R-Smad and I-Smad targets (Fig. 1). Intriguingly, only the second of two Smurf1 WW domains (Smurf1 WW2) and the third of three Smurf2 WW domains (Smurf2 WW3) are competent for PY-motif ligand binding in isolation (6, 14). Still, both the WW2 and WW3 of Smurf2 are required for optimal target recognition implying that they cooperate (9).

Neither the WW2 nor the WW3 of Smurf2 is canonical (Fig. 1). Smurf2 WW2 and the homologous WW1 of Smurf1 have a tyrosine at the site normally occupied by the conserved core tryptophan, which likely destabilizes these domains. Smurf2 WW3 and the homologous Smurf1 WW2 do not have the highly conserved binding site tryptophan, which interacts with the prolines of target PY motifs. The structure of Smurf2 WW3 bound to a peptide derived from the PY-motif region of Smad7 (S7PY) revealed that in addition to binding the PY motif, the WW3 domain binds to the PY tail, which is comprised of the six residues C-terminal to the PY motif (14). The PY tail compensates for the drop in affinity due to the lack of a binding site tryptophan. Several mechanisms can be envisioned by which Smurf2 WW2 might enhance the affinity of the WW3 for target PY motifs. The WW2 might bind to regions N- or C-terminal to the PY motif. The third β-strand of WW3 might be swapped for the third β-strand of WW2, which has the canonical tryptophan. The WW3 might also stabilize the WW2 making it competent to bind PY-motif ligands.

The degree and mechanism of ligand selectivity by modular binding domains is of critical interest because of its predictive value in deciphering biological pathways. Here we present structural and binding studies aimed at determining how the Smurf2 WW2 enhances the affinity of Smurf2 for Smad PY motif-containing peptides. Binding experiments demonstrate that Smurf2 WW23, a construct containing both the WW2 and WW3 domains of Smurf2 in tandem, has a higher affinity for S7PY relative to the

Author contributions: P.A.C. and J.D.F.-K. designed research; P.A.C. and H.L. performed research; P.A.C. and H.L. contributed new reagents/analytic tools; P.A.C. analyzed data; and P.A.C., J.L.W., and J.D.F.-K. wrote the paper.

The authors declare no conflict of interest.

This article is a PNAS Direct Submission.

Freely available online through the PNAS open access option.

Data deposition: The atomic coordinates and NMR chemical shifts and restraints have been deposited in the Research Collaboratory for Structural Bioinformatics (RCSB) Protein Data Bank, www.pdb.org (PDB ID code 2KXQ and RCSB ID code RCSB101704).

[1]To whom correspondence should be addressed. E-mail: forman@sickkids.ca.

This article contains supporting information online at www.pnas.org/lookup/suppl/doi:10.1073/pnas.1003023107/-/DCSupplemental.

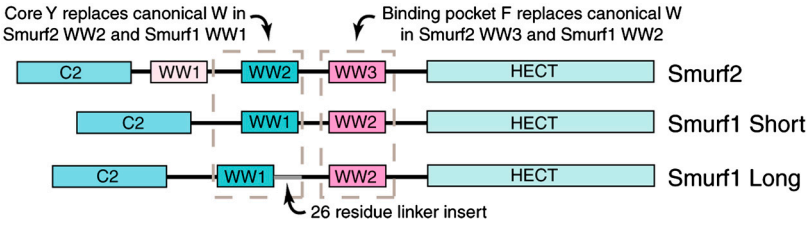


**Fig. 1.** Schematic diagram of Smurf2 and Smurf1 Short and Long. The analogous Smurf2 WW2 and Smurf1 WW1 domains have a core tyrosine instead of the canonical tryptophan. The analogous Smurf2 WW3 and Smurf1 WW2 domains have a binding pocket phenylalanine instead of the canonical tryptophan. The Long Smurf1 isoform has an extended inter-WW domain linker.

isolated WW3. The solution structure of a Smurf2 WW23:S7PY complex reveals that the WW2 binds to the WW3 and also binds to the Smad7 PY motif and residues N-terminal to the PY motif. These results highlight the potential for expanding target recognition surfaces to enhance specificity by assembly of modular domains into a composite domain. In addition, the observed decrease in Smad PY peptide binding affinity with increase in Smurf1 inter-WW domain linker length identifies a mechanism by which isoform switching tunes Smurf:Smad binding affinity.

## Results

**Smurf2 WW2 Enhances the Interaction Between S7PY and Smurf2 WW3.** Although the isolated WW3 of Smurf2 binds to S7PY and the isolated WW2 of Smurf2 does not (14), immunoprecipitation experiments indicate that both the WW2 and WW3 are required for optimal binding of Smad targets (9). To assess whether a protein containing both of these domains of Smurf2 in tandem (Smurf2 WW23) has a higher affinity for S7PY than the isolated WW3, intrinsic tryptophan fluorescence was used to measure the affinity of WW23 for S7PY. The dissociation constant for the WW23:S7PY interaction was found to be $1.7 \pm 0.4$ μM (Fig. S1 and Table S1), reflecting ~20-fold higher affinity than for the WW3:S7PY interaction. To explore the origins of this enhanced affinity, heteronuclear single quantum correlation (HSQC) spectra of WW23 in the presence of saturating amounts of S7PY were recorded and compared to spectra of WW3 bound to S7PY and spectra of the WW2 (Fig. 2 and Fig. S2*a*). The peaks on the HSQC arise primarily from backbone amides, and their peak positions are dependent on the immediate chemical environment of each amide group. Changes in peak position thus indicate a change in structure or dynamics. Because the WW2 does not bind S7PY, no peak shifts were observed upon addition of S7PY to the WW2 (14). However, spectral changes were observed upon addition of S7PY peptide to either the isolated WW3 or the WW23 tandem. Comparing spectra of WW3 in the presence of saturating S7PY peptide (blue) to that of WW23:S7PY complex (red), we observed that the chemical shifts of many of the WW3 residues differed significantly. Thus, within the tandem WW23, the WW3 does not bind independently to the PY motif of S7PY; otherwise, only minor changes to peaks corresponding to the WW3 portion of the protein would be expected. This suggests an interaction between the WW2 and the WW3. Indeed, peaks corresponding to the WW2 in the WW23:S7PY spectra also shifted extensively when compared to the spectra of the isolated WW2 (green). These WW2 changes might reflect stabilizing interactions with S7PY and/or WW3.

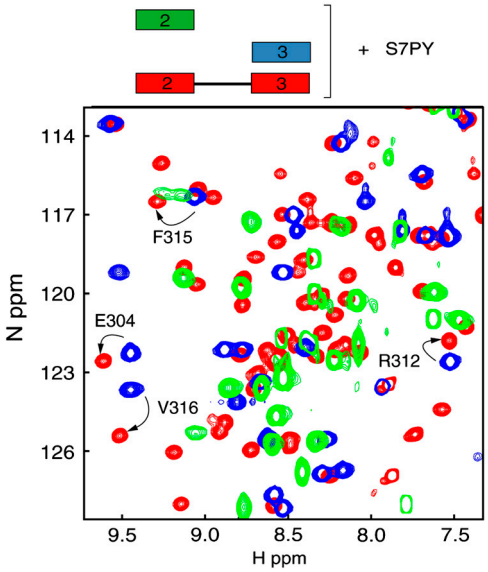


**Fig. 2.** Tandem Smurf2 WW23 uses an altered S7PY binding mechanism compared to the isolated WW3. Superposition of a portion of Smurf2 WW2 (green), WW3 (blue), and WW23 (red) $^{1}$H-$^{15}$N HSQC spectra recorded in the presence of S7PY. Peak shifts are labeled for several residues.

**Solution Structure of Smurf2 WW23 Bound to S7PY.** To provide insight into the enhanced affinity of the tandem WW23, full resonance assignments for the WW23 in complex with S7PY were obtained and a solution structure determined using NMR-derived distance and orientation restraints (Fig. 3 *A* and *C* and Fig. S3). The resultant structural ensemble is well defined for residues 253–329 of Smurf2 and residues 205′–217′ of Smad7 (here we use ′ to distinguish PY peptide residues from WW domain residues), with an overall backbone rmsd of $0.74 \pm 0.16$ Å and lower rmsd values for the individual domains (Table S2). The structure revealed that both WW domains form the typical WW fold. Notably, an extensive interface between the WW2 and both the WW3 and S7PY was observed. The second and third β-strands of the WW2 pack against the third β-strand of the WW3, with the strands of the two domains oriented approximately perpendicular to each other. Over 70 inter-WW domain NOEs were observed (Table S2), indicating that the WW2-WW3 interaction is stable in the presence of S7PY.

To measure the backbone mobility of the various regions of the WW23:S7PY complex, heteronuclear NOE data were recorded on a $^{15}$N labeled sample (Fig. 3*B*). The amide groups within WW2 and WW3 are the least dynamic having NOE ratios between 0.7 and 0.8, with the loop between the second and third β-strands of WW2, the loop between the first and second β-strands of WW3 and the amide groups in the interdomain linker having lower NOE ratios indicating greater mobility. However, they are not as mobile as the N and C termini of the WW23 construct, which had negative NOEs. Amide groups within the Smad7 peptide displayed a range of mobility, with residues between E205′ and Y214′ having positive heteronuclear NOE ratios, indicating some restriction of motion. Altogether, these data indicate that, in the presence of S7PY, the WW2 and WW3 form a stable interaction with restricted interdomain linker motion. Additionally, the coupled WW domains form an interaction with the S7PY peptide that restricts the motion of 10 Smad7 residues.

**Smurf2 WW2 Is Unstable and Unable to Bind PY Motifs.** To probe the molecular basis for the inability of the isolated WW2 of Smurf2 to bind S7PY, the structure of the WW2 within the complex was examined for key stability and PY-motif binding features. When compared to the crystal structure of the dystrophin WW domain, two critical elements were found to differ (Fig. 4*A*). First, the residue at the canonical core tryptophan position (W3061 in dystrophin), which is required for WW domain stability (2), is

BIOCHEMISTRY

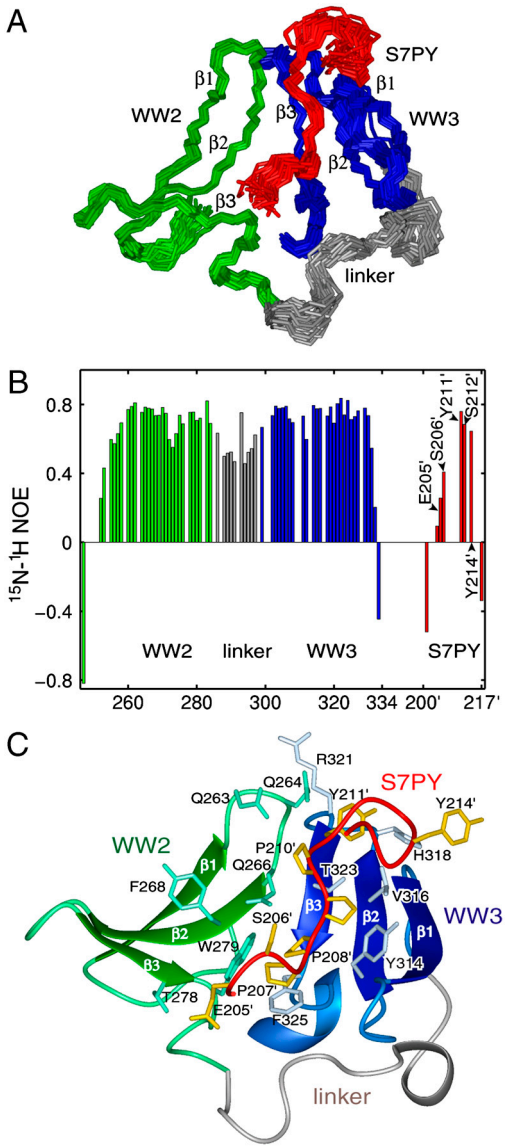


**Fig. 3.** Solution structure of Smurf2 WW23 tandem bound to S7PY. (*A*) Backbone superposition of the 30 lowest energy structures. The WW2, the interdomain linker and the WW3 are shown in green, gray, and blue, respectively. S7PY (sequence: ELESPPPPYSRYPMD) is shown in red. (*B*) $^{1}$H-$^{15}$N heteronuclear NOE values for residues in the complex are shown with the same color scheme as in *A*. Numbers along the x axis with and without the primes indicate Smad7 and Smurf2 residue numbering, respectively. (*C*) Ribbon diagram of the complex. The WW2, linker, and WW3 are shown in green, gray, and blue, respectively. The backbone of S7PY is shown in red, whereas the side chains are in yellow. For clarity most side chains are not shown. Smad7 residues are labeled with the prime symbol.

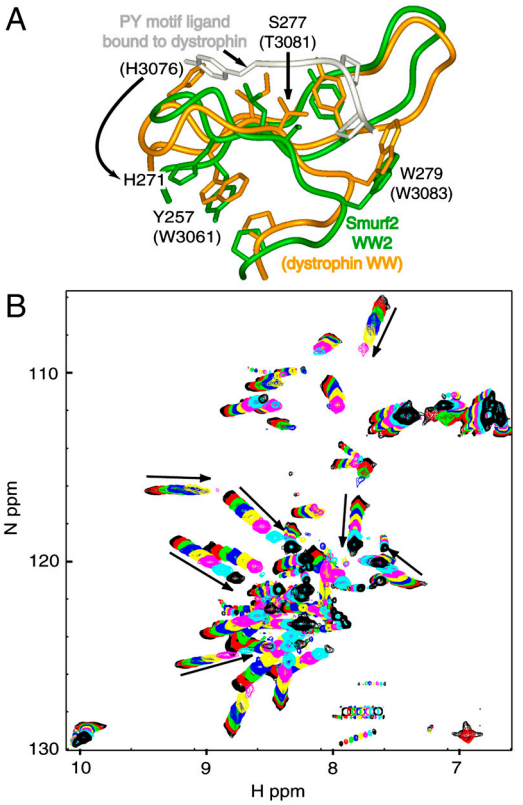


**Fig. 4.** Smurf2 WW2 is impaired in PY-motif recognition and stability. (*A*) Superposition of ribbon diagrams of the Smurf2 WW2 (green) from the solution structure of the complex and of the dystrophin WW domain, a representative group I WW domain (gold) (26). The dystrophin WW domain's PY-motif ligand is shown in gray. For clarity most side chains are not shown. Labels in parentheses indicate dystrophin WW domain residues. (*B*) Overlay of $^{1}$H-$^{15}$N HSQC spectra recorded at 5 °C (black), 10 °C (red), 15 °C (green), 20 °C (blue), 25 °C (yellow), 30 °C (magenta), 35 °C (cyan), and 40 °C (black). Arrows indicate the peak movement with increasing temperature.

a tyrosine (Y257) in Smurf2. To examine the stability of the WW2 containing this tyrosine, HSQC spectra of the isolated WW2 were recorded at various temperatures. As temperature increased the peaks became progressively less dispersed in the amide proton dimension, migrating from folded to random coil positions (Fig. 4*B*). This progressive movement of peaks is diagnostic of a fast exchange process. The direction of the movement from folded to random coil values indicated that the exchange process was likely between a folded and an unfolded state. Thus the isolated WW2 appears to rapidly exchange ($>10^{6}$ $s^{-1}$) between a folded and an unfolded state with the population of unfolded WW2 increasing at higher temperatures. Thermal melts of WW2 monitored by CD spectroscopy indicated an unfolding midpoint of 36.1 ± 1.5 °C (Fig. S4 *a* and *b*). Second, the structure showed that two residues critical for PY-motif binding are missing from the binding surface (Fig. 4*A*). The histidine residue (H271 in Smurf2, H3076 in dystrophin) normally found at the end of the second β-strand of group I WW domains is flipped onto the opposite side of the β-sheet. This histidine normally forms a critical part of the tyrosine binding pocket (3). Finally, the well-conserved threonine on the third β-strand, which forms a hydrogen bond with a PY-motif backbone carbonyl in many group I WW domain-peptide structures (3) (T3081 in dystrophin), is a serine in Smurf2 WW2 (S277). Collectively, these data provide a basis for the failure of the isolated WW2 to bind to S7PY.

**Both the WW2 and the WW3 Contribute to S7PY Binding.** The isolated WW2 is unstable and fails to bind PY motifs. However, it contributes to overall tandem WW23 affinity for S7PY and makes extensive contacts with WW3. Both CD and NMR data show that the WW2 does not significantly stabilize the WW3 either *in cis* or *in trans* (see Fig. S4 and discussion thereof in *SI Text*). The inter-WW domain linker may stabilize the WW3 and may enhance binding of the S7PY peptide (Table S1), but the data indicate that the presence of the WW2 is required for the full 20-fold boost in affinity. Therefore, we examined the tandem structure for insight into how WW2 enhances affinity for S7PY. The WW3 forms the primary contacts with the S7PY peptide. The PY motif and PY tail, formed by the six residues C-terminal to the PY motif, bind in a conformation that is similar to their interaction with the isolated WW3 (14). The backbone rmsd between the isolated

and tandem forms is 1.24 Å for Smurf2 WW3 (299–329) and Smad7 (208′–214′), with the biggest differences observed in the flexible loop between the first and second β-strands of WW3 and the flexible C-terminus of S7PY. The tyrosine of the PY motif, Y211′, lies in the hydrophobic pocket formed by V316, H318, and R321 (Fig. 3*C* and Fig. S3). The PY tail loops around and binds residues on the first and second β-strands of WW3 and is stabilized by intrapeptide interactions. The WW2 forms additional contacts with the prolines of the PY motif (P208′–P210′) and the proline preceding the PY motif (P207′). P207′ and P208′ nestle in a pocket formed by WW2 residues W279 and Q266 and WW3 residues T323 and F325 (Fig. 3*C*). P210′ binds in a pocket formed by three WW2 glutamines, Q263, Q264, and Q266. E205′ and S206′, which are N-terminal to the PY motif, interact with W279, although as the heteronuclear NOE data indicates (Fig. 3*B*) they are flexible and likely sample multiple conformations. The WW domain coupling places W279 of WW2 directly opposite the position normally occupied by the binding pocket tryptophan of WW3, where it functions to compensate for the lack of this binding pocket tryptophan. Altogether the data imply that WW2 contributes to the enhanced affinity of the tandem WW23 for S7PY by forming additional contacts with the prolines of the PY motif and residues N-terminal to the PY motif.

The WW3 affinity for S7PY is enhanced by an interaction between the WW3 and residues C-terminal to the PY motif (14). To probe whether the flexible residues N-terminal to the PY motif, E205′ and S206′, contribute energetically to S7PY binding, we made single alanine mutations at these positions and measured the affinity of Smurf2 WW23 for these mutant S7PY peptides using fluorescence. Dissociation constants of $2.5 \pm 0.2$ and $1.6 \pm 0.3$ μM were measured for E205′A and S206′A, respectively (Fig. S1 and Table S1). The slightly reduced affinity of WW23 for E205′A S7PY relative to WT, suggests that the glutamic acid residue in position 205′ makes a small energetic contribution to the interaction. Mutation of S206′ to alanine had little effect on the binding affinity, suggesting either that alanine is a good substitute for the serine or that S206′ makes a minimal contribution. Thus the binding data suggest that the E-S-P sequence immediately N-terminal to the Smad7 PY motif makes a minor energetic contribution to the interaction.

**Smad1 and Smad2 Peptides Are Also Recognized by Smurf2 Using the Coupled WW Domain Configuration.** An alignment of Smad proteins revealed that the sequence E/D-S/T-P precedes all of the Smad PY motifs (Fig. S5*a*). To confirm that Smurf2 WW23 can bind the PY motifs of Smad1 and Smad2, representative bone morphogenetic protein and TGF-β responsive R-Smads, respectively, HSQC NMR was used to monitor addition of unlabeled Smurf2 WW23 into $^{15}$N labeled PY motif-containing peptides derived from Smad1 and Smad2 (S1PY and S2PY) (Fig. S6 *a* and *b*). In both cases many peak shifts and changes in relative peak intensity were observed confirming that these peptides bind to Smurf2 WW23. The number of shifts indicates that regions beyond the PY motifs of these proteins interact with Smurf2 WW23. Together the binding and alignment data demonstrate that Smurf2 WW23 also binds to Smad1 and Smad2 peptides and suggest that the interaction of the E/D-S/T-P sequence with the WW2 serves as a specific marker for Smad recognition by Smurf2.

To directly test whether Smurf2 binds to Smad1 and Smad2 using the coupled WW domain mechanism, HSQC spectra of $^{15}$N labeled Smurf2 WW23 were recorded with saturating amounts of S1PY or S2PY and compared to spectra of Smurf2 WW23 bound to S7PY. The chemical shifts of Smurf2 WW3 resonances, especially resonances from the third β-strand that interacts with the WW2 domain, differ greatly depending on whether the WW2 is interacting with the WW3 or not (i.e., isolated WW3 vs. tandem WW23) (Fig. 5*D*). Comparing the S7PY-bound WW3, S1PY-bound WW23, and S2PY-bound WW23 to S7PY-bound Smurf2 WW23 gave average chemical shift differences of 9.55, 1.70, and 1.67 Hz, respectively, for 19 shared residues that were assigned in all four complexes (Fig. 5*E*). As shown, chemical shifts for the third β-strand of the WW3 in the case of Smurf2 WW23 bound to either Smad1 or Smad2 (Fig. 5 *A* and *B*) were similar to those observed for the WW23:S7PY complex. The similarity of the third β-strand chemical shifts for the tandem WW23 bound to S1PY, S2PY, and S7PY confirms that both Smad1 and Smad2 are recognized via the coupled WW configuration used to bind Smad7. Collectively, the structural, binding, and sequence conservation data support a conserved mechanism for recognition of the Smad proteins by coupled tandem WW domains of Smurf2, in which the WW2 enhances the interaction affinity by forming auxiliary contacts with the prolines of the PY motif in addition to the primary interactions these prolines form with the WW3 and by binding to the Smad E/D-S/T-P sequence.

**The Inter-WW Domain Linker Length Alters the S7PY Interaction of Expressed Smurf1 Isoforms.** Because Smurf1 and Smurf2 share a number of PY-motif-containing substrates, the sequences were compared to determine whether Smurf1 recognizes its substrates using the same coupled WW domain mechanism. Smurf1 has only WW1 and WW2 domains, which are highly similar to the WW2 and WW3 of Smurf2, respectively (Fig. 1 and Fig. S5*b*), suggesting that Smurf1 binds to PY-motif-containing proteins using the same mechanism as Smurf2. Smurf1 is expressed in two isoforms. The shorter isoform (Short) has an inter-WW domain linker that is the same length as the corresponding Smurf2 linker. We recorded spectra of S7PY-saturated Short Smurf1 WW1 and WW2 in tandem (WW12) and compared this to spectra of S7PY-bound Smurf2 WW23. Comparison of the chemical shifts of the same 19 shared residues discussed in the previous paragraph yielded an average chemical shift difference of only 2.29 Hz, with the largest differences occurring spatially near to positions that have sequence differences between Smurf1 and Smurf2 (Fig. 5 *C* and *E*). The similarity of the chemical shifts, particularly for amide groups within the third β-strand, confirms that Smurf1 uses the same coupled WW domain mechanism to recognize S7PY.

Alternative splicing of Smurf1 results in expression of a longer isoform (KIAA1625, Long), which has 26 additional inter-WW domain linker residues. In the Smurf2 WW23:S7PY structure, the WW domain linker forms close contacts with the face of the WW3 β-sheet that is opposite to the PY-motif binding face. The linker has restricted motion as indicated by the number of NOEs between the linker and the WW3 and the heteronuclear NOE data (Fig. 3*B*). The N terminus of the linker precisely positions the WW2 (equivalent to Smurf1 WW1) to cooperate in the S7PY interaction. Thus we hypothesized that the extra residues in the Long Smurf1 isoform, which are inserted between WW1 and the N terminus of the short linker (Fig. 1), might alter the mechanism by which this protein binds to PY-motif targets. Therefore we compared the spectra of S7PY-bound states of Long Smurf1 WW12 to S7PY-bound Short Smurf1 WW12, which uses the coupled WW domain binding mechanism, and to S7PY-bound Short Smurf1 linker-WW2, in which the WW2 independently binds to S7PY. S7PY-bound Long Smurf1 WW12 protein spectra exhibit significant resonance broadening due to conformational exchange and/or aggregation. The WW2 resonances of Long Smurf1 WW12 do not coincide completely with either Short Smurf1 WW12 or Short Smurf1 linker-WW2, but rather lie between these two extremes (Fig. 6 and Fig. S7), suggesting that the WW2 binds to S7PY in both an independent and a WW1 bound format. Residues affected by the longer linker include some in the WW2:S7PY and WW2:WW1 interaction surfaces, which are distant from the linker interaction surface,

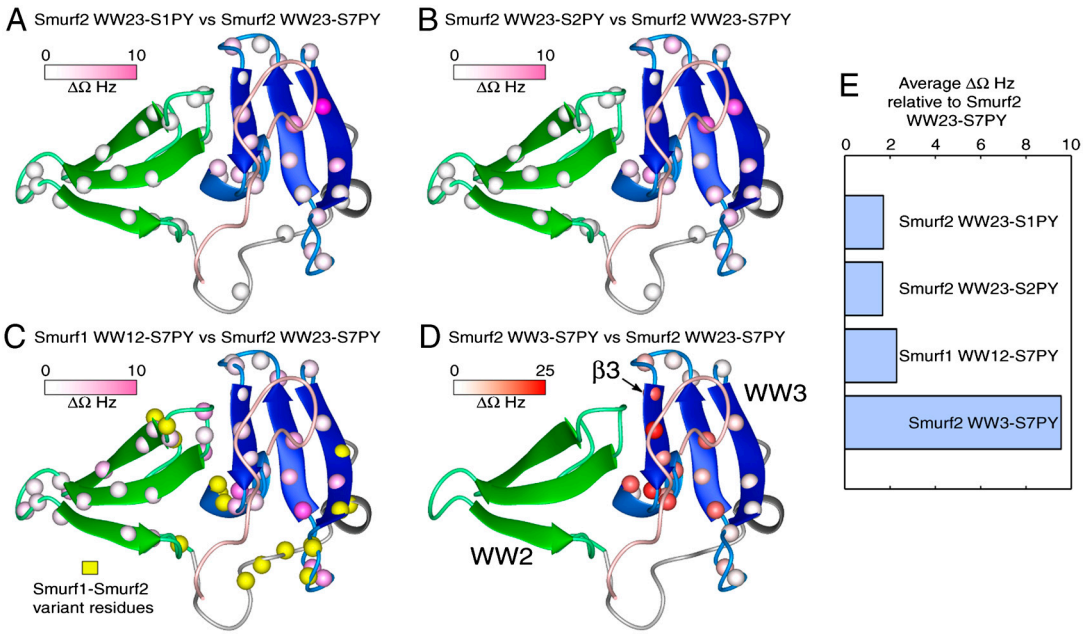


**Fig. 5.** Comparison of chemical shift differences between the Smurf2 WW23:S7PY reference complex and the Smurf2 WW23:Smad1 PY complex, the Smurf2 WW23:Smad2 PY complex, the Smurf1 WW12:S7PY complex, and the Smurf2 WW3:S7PY complex. (*A–D*) Chemical shift differences between different protein complexes were calculated as $\Delta\Omega = [(\Delta\Omega_{nit})^2 + (\Delta\Omega_{prot})^2]^{1/2}$, where $\Delta\Omega_{nit}$ and $\Delta\Omega_{prot}$ are the differences in the nitrogen and proton chemical shift in Hz. Differences between each complex and the Smurf2 WW23:S7PY complex were mapped onto ribbon diagrams of Smurf2 WW23 for assigned residues in each complex. The size of the differences was mapped onto spheres representing the backbone nitrogen atoms using a color gradient. The scaling is as shown in each panel. Sequence positions that have different residues in Smurf1 and Smurf2 are represented as yellow spheres at the nitrogen atom location. The Smurf2 WW2, interdomain linker and WW3 and the Smad7 PY peptide are shown in green, gray, blue, and light pink, respectively. (*A*) Plot of the average chemical shift difference between each complex and the reference complex, Smurf2 WW23:S7PY, for 19 residues assigned in all of the complexes.

indicating that the S7PY binding mechanism is affected and not just the linker interaction. Together with broadened linewidths, the data suggest that the Long Smurf1 WW12:S7PY complex exchanges between WW1 bound and unbound states at an intermediate rate on the NMR time scale (ms-μs). Although the Short Smurf1 WW12 appears close to saturation with S7PY at a 1:1 ratio, the longer isoform is not saturated even with a 10-fold excess of S7PY. Thus the longer linker decreased the affinity of Long Smurf1 for S7PY.

## Discussion

We have shown that when the WW2 and WW3 of Smurf2 are in tandem, they stably couple to jointly bind a Smad7 peptide. Within the tandem context, the WW3 binds to the PY motif in almost the same way as the independent WW3 does. However the WW2 makes auxiliary contacts with the PY motif and binds to an E/D-S/T-P motif N-terminal to the PY motif enhancing the affinity of Smurf2 for Smad7 over 20-fold, thereby explaining the requirement for both WW domains. Smurf2 WW23 also binds to PY motifs from Smad1 and 2, which share the same E/D-S/T-P motif. The shorter Smurf1 isoform also utilizes the coupled WW domain mechanism to bind to Smad7, whereas the longer Smurf1 isoform likely uses both the isolated WW2 and the coupled WW12 to bind to Smad7. The conservation between Short Smurf1 WW12 and Smurf2 WW23 and the common use of the coupled binding mechanism provide a mechanistic basis for the overlapping specificities of Smurf1 and Smurf2 (15).

WW domain clustering results in a variety of tertiary interactions, which refine their function. For example, FBP11's two consecutive WW domains likely enable simultaneous binding to two polyproline target motifs in formin homology 1 regions, enhancing the affinity of this interaction (7). The two WW domains of Prp40 are joined by a stable α-helical linker that fixes the relative orientation of the WW domains, such that their binding pockets face in opposite directions (16). This may enable the Prp40 WW domains to interact simultaneously with two proline-rich target sites and function as an adapter. The WW3 of suppressor of deltex [Su(dx)] interacts with the Su(dx) WW4 domain inhibiting the WW4 from binding to a Notch-PY motif (17, 18). Binding of a ligand to the Su(dx) WW3 stabilizes it and reduces its inhibitory interactions with the WW4. Thus the Su(dx) WW3 enables context-dependent regulation of WW4 target binding. In contrast, the WW domains of Smurf1 and Smurf2 have a joint binding surface that enhances target selectivity. Unlike the WW3 of Su(dx), the WW2 of Smurf2 functions to enhance the interaction of the Smurf2 WW3 with its target and is likely incapable of binding to

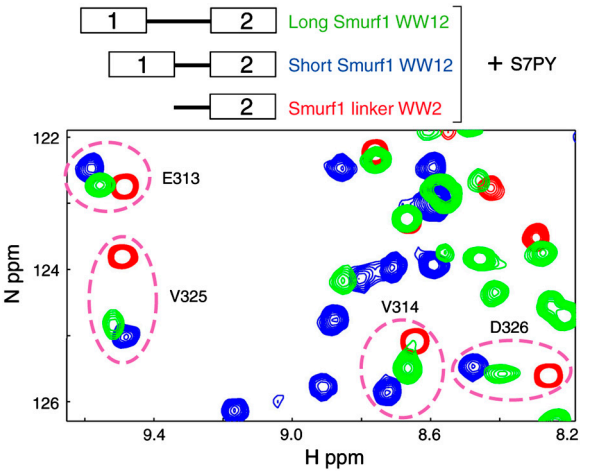


**Fig. 6.** The WW2 of Long Smurf1 WW12 binds to S7PY in both an independent and a WW1 bound format. Overlay of a portion of the $^{1}H$-$^{15}N$ HSQC spectra of Short Smurf1 WW12:S7PY (blue), Short Smurf1 linker-WW2:S7PY (red) and Long Smurf1 WW12:S7PY (green) complexes. Peaks representing the same residues in the different complexes are circled and identified. See Fig. S7 for the full HSQC overlay. Identified residues shown here and in Fig. S7 are located on the three β-strands of the WW2 domain.

target peptides in isolation. Phosphorylation of the conserved binding pocket threonine, T30, of the Itch WW3 domain inhibits binding of PY-motif-containing ligands (19). As the equivalent threonine residues in Smurf1 and Smurf2 (T331 Smurf1 and T323 Smurf2; see Fig. 3*C*) are at the inter-WW domain interface, phosphorylation would likely lead to a dramatic reduction in affinity for the Smad proteins. The coupled Smurf WW binding mechanism may allow the interaction with the Smad proteins to be disrupted by phosphorylation. Similarly, our results provide a basis for explaining how phosphorylation of the threonine in the E/D-S/T-P motifs of Smad2 and Smad3 modulates their interactions with Smurf1's WW1 and Smurf2's WW2, in addition to modulating interaction with Nedd4L (20). Thus interactions between adjacent WW domains introduce added complexity to their function.

The length and structure of the interdomain linkers also appear to be crucial. The short linker joining the last two WW domains of Smurf2 facilitates WW domain coupling upon peptide binding. The increased linker length in the longer Smurf1 isoform reduces the affinity of the WW domains for each other and for S7PY and alters the binding mechanism, suggesting that alternative splicing provides a mechanism for altering Smurf1 specificity. Many examples of inter-WW domain linker conservation exist (see examples in Fig. S5*b*). Short conserved linkers suggest a requirement for interaction between the WW domains. One interesting example is hWWP2 and hItch, which have no linker between the first two WW domains, suggesting that they are fused into a super-WW domain structure. Linker conservation may also be due to a requirement for an accessory protein binding site in the linker. For example, casein kinase-2 interacting protein-1 (CKIP-1) has been shown to bind the Smurf1 linker and enhance Smurf1 affinity for Smad5 and 7 (21). We speculate that CKIP-1 functions to increase Smurf1 affinity by stabilizing the WW domain coupling. Thus linker length and interactions between the interdomain linker and accessory proteins provide additional regulation of Smurf WW domain activity.

We have found a unique mechanism by which clustered WW domains provide for specific adaptable recognition of the Smad proteins by Smurf1 and Smurf2. Smurf2 forms numerous intra- and intermolecular regulatory interactions. Autoinhibition of Smurf2 is achieved by an interaction between the N-terminal C2 domain and the HECT domain, likely preventing premature autoubiquitination in the absence of appropriate substrates (22). The N-terminal domain of Smad7 competes with the C2 for binding to the HECT domain relieving autoinhibition. Smad7 also promotes Smurf2 catalytic activity by recruiting an E2 ubiquitin conjugating enzyme (23) and substrates, such as the TGF-β receptor complex (9). The modular domains of Smurf1 and Smurf2 do not behave like beads on a string; instead many critical intra and intermolecular interactions work in concert to regulate function.

## Methods

**Protein and Peptide Preparation.** DNA constructs encoding the Smurf2 WW2 (aa 250–288), WW3 (aa 297–333), and WW2 and WW3 domains in tandem (Smurf2 WW23, aa 250–333) were used to prepare Smurf2 derived proteins (Fig. 2). DNA constructs encoding the Smurf1 inter-WW domain linker and WW2 domain (Smurf1 linker-WW2, aa 294–342), the Smurf1 WW2 domain (aa 306–342) and the Long and Short forms of Smurf2 WW1 and WW2 in tandem (Long Smurf1 WW12, aa 234–342; Short Smurf1 WW12, aa 234–268 and 294–342), were used to prepare Smurf1-derived proteins (Fig. 6). Peptides corresponding to the PY-motif regions of Smad1, 2 and 7 (S1PY—Smad1, aa 215–236; S2PY—Smad2, aa 214–233; and S7PY—Smad7, aa 203–217) were prepared using standard Fmoc chemistry or expressed recombinantly for labeling purposes. For more details, see *SI Methods*.

**NMR Spectroscopy Methods.** Experiments were performed at 25 °C in 40 mM $Na_2HPO_4$, pH 7.2, 20 mM NaCl, 1 mM EDTA, 0.05% $NaN_3$, 0.5 mM benzamidine and 10% $D_2O$. Standard experiments were used to assign the backbone and side-chain resonances (24) of both Smurf2 WW23 and the S7PY peptide in the bound state, using a sample in which both polypeptides were $^{15}N$ and $^{13}C$ labeled. The structure was calculated using a combination of automated and manual methods using NOE data, chemical shift derived angular restraints, and residual dipolar coupling data. See *SI Methods* for more details.

**Binding Studies.** Fluorescence binding experiments were performed at 20 °C in buffer containing 40 mM $Na_2HPO_4$, pH 7.2, and 20 mM NaCl and 1 mM fresh β-mercaptoethanol. Fluorescence levels were monitored as peptide was added to the WW23 protein samples and data was fit as previously published (25). See *SI Methods* for more details.

**ACKNOWLEDGMENTS.** We thank Drs. R. Muhandiram for help with NMR experiments and R. Hudson, V. Kanelis, A. Velyivus, S. Wiesner, and R. Sprangers for useful discussions. We acknowledge funding from the Canadian Institute for Health Research (to J.L.W.) and the Canadian Cancer Society (to J.D.F.-K.). J.L.W. is an International Scholar of the Howard Hughes Medical Institute and a Canada Research Chair in Systems Biology.

1. Ingham RJ, Gish G, Pawson T (2004) The Nedd4 family of E3 ubiquitin ligases: Functional diversity within a common modular architecture. *Oncogene* 23:1972–1984.
2. Koepf EK, et al. (1999) Characterization of the structure and function of *W → F* WW domain variants: Identification of a natively unfolded protein that folds upon ligand binding. *Biochemistry* 38:14338–14351.
3. Macias MJ, Wiesner S, Sudol M (2002) WW and SH3 domains, two different scaffolds to recognize proline-rich ligands. *FEBS Lett* 513:30–37.
4. Bhattacharya S, Zoladek T, Haines DS (2008) WW domains 2 and 3 of Rsp5p play overlapping roles in binding to the LPKY motif of Spt23p and Mga2p. *Int J Biochem Cell Biol* 40:147–157.
5. Kanelis V, Rotin D, Forman-Kay JD (2001) Solution structure of a Nedd4 WW domain-ENaC peptide complex. *Nat Struct Biol* 8:407–412.
6. Otte L, et al. (2003) WW domain sequence activity relationships identified using ligand recognition propensities of 42 WW domains. *Protein Sci* 12:491–500.
7. Ramirez-Espain X, Ruiz L, Martin-Malpartida P, Oschkinat H, Macias MJ (2007) Structural characterization of a new binding motif and a novel binding mode in group 2 WW domains. *J Mol Biol* 373:1255–1268.
8. Li Y, Zhou Z, Alimandi M, Chen C (2009) WW domain containing E3 ubiquitin protein ligase 1 targets the full-length ErbB4 for ubiquitin-mediated degradation in breast cancer. *Oncogene* 28:2948–2958.
9. Kavsak P, et al. (2000) Smad7 binds to Smurf2 to form an E3 ubiquitin ligase that targets the TGF beta receptor for degradation. *Mol Cell* 6:1365–1375.
10. Zhu H, Kavsak P, Abdollah S, Wrana JL, Thomsen GH (1999) A SMAD ubiquitin ligase targets the BMP pathway and affects embryonic pattern formation. *Nature* 400:687–693.
11. Attisano L, Wrana JL (2002) Signal transduction by the TGF-beta superfamily. *Science* 296:1646–1647.
12. Shi Y, Massague J (2003) Mechanisms of TGF-beta signaling from cell membrane to the nucleus. *Cell* 113:685–700.
13. Hayashi H, et al. (1997) The MAD-related protein Smad7 associates with the TGFbeta receptor and functions as an antagonist of TGFbeta signaling. *Cell* 89:1165–1173.
14. Chong PA, Lin H, Wrana JL, Forman-Kay JD (2006) An expanded WW domain recognition motif revealed by the interaction between Smad7 and the E3 ubiquitin ligase Smurf2. *J Biol Chem* 281:17069–17075.
15. Inoue Y, Imamura T (2008) Regulation of TGF-beta family signaling by E3 ubiquitin ligases. *Cancer Sci* 99:2107–2112.
16. Wiesner S, Stier G, Sattler M, Macias MJ (2002) Solution structure and ligand recognition of the WW domain pair of the yeast splicing factor Prp40. *J Mol Biol* 324:807–822.
17. Fedoroff OY, Townson SA, Golovanov AP, Baron M, Avis JM (2004) The structure and dynamics of tandem WW domains in a negative regulator of notch signaling, Suppressor of deltex. *J Biol Chem* 279:34991–35000.
18. Jennings MD, Blankley RT, Baron M, Golovanov AP, Avis JM (2007) Specificity and autoregulation of Notch binding by tandem WW domains in suppressor of Deltex. *J Biol Chem* 282:29032–29042.
19. Morales B, et al. (2007) NMR structural studies of the ItchWW3 domain reveal that phosphorylation at T30 inhibits the interaction with PPxY-containing ligands. *Structure* 15:473–483.
20. Gao S, et al. (2009) Ubiquitin ligase Nedd4L targets activated Smad2/3 to limit TGF-beta signaling. *Mol Cell* 36:457–468.
21. Lu K, et al. (2008) Targeting WW domains linker of HECT-type ubiquitin ligase Smurf1 for activation by CKIP-1. *Nat Cell Biol* 10:994–1002.
22. Wiesner S, et al. (2007) Autoinhibition of the HECT-type ubiquitin ligase Smurf2 through its C2 domain. *Cell* 130:651–662.
23. Ogunjimi AA, et al. (2005) Regulation of Smurf2 ubiquitin ligase activity by anchoring the E2 to the HECT domain. *Mol Cell* 19:297–308.
24. Kanelis V, Forman-Kay JD, Kay LE (2001) Multidimensional NMR methods for protein structure determination. *IUBMB Life* 52:291–302.
25. Chong PA, Ozdamar B, Wrana JL, Forman-Kay JD (2004) Disorder in a target for the smad2 mad homology 2 domain and its implications for binding and specificity. *J Biol Chem* 279:40707–40714.
26. Huang X, et al. (2000) Structure of a WW domain containing fragment of dystrophin in complex with beta-dystroglycan. *Nat Struct Biol* 7:634–638.